Energy band structure of Bi-$Bi_{1-x}Sb_x$ compositional superlattices

1994 J. Phys.: Condens. Matter 6 2039

(http://iopscience.iop.org/0953-8984/6/10/021)

J. Phys.: Condens. Matter 6 (1994) 2039–2046. Printed in the UK

Energy band structure of Bi–$Bi_{1-X}Sb_X$ compositional superlattices

N B Mustafaev

Institute of Physics, Academy of Sciences of Azerbaijan, H Cavid Prospekti 33, Baku, Azerbaijan

Received 1 October 1993

Abstract. Within the McClure model a dispersion equation for the energy spectrum of the Bi–$Bi_{1-X}Sb_X$ superlattices in the envelope function approximation is derived. The effective mass of minibands, the Fermi energy and the concentration of free carriers in a superlattice with $X = 0.1$ and the period $d = 10$ nm are determined. The dependence of the miniband energy upon the ratio $r = d^{I}/d^{II}$ is obtained (d^{I} is the thickness of the Bi layers and d^{II} is the thickness of the alloy layers). It is shown that there is a transition from the semiconducting state ($r < 0.31$) to the semimetallic state ($r > 0.31$) in the superlattice with $X = 0.1$ and $d = 10$ nm due to an energy overlap between the minibands at the L and T points of the Brillouin zone. For $d^{I} = 4$ nm and $d^{II} = 6$ nm the Fermi surface of electrons is closed whereas the Fermi surface of holes is open in the direction of the superlattice wavevector q. In the superlattice with $X = 0.12$ and $d^{I} = d^{II} = 60$ nm the transverse components of the effective-mass tensor change signs at a certain value of $q = q_0$. As a result, at $q > q_0$ the dependence of the miniband energy on the wavevector k in the plane of layers has a shape like a 'camel's back'.

1. Introduction

The Bi/Sb multilayered structures [1] are of great interest at present. Galvanomagnetic effects [2] and the Aharonov–Bohm effect [3] were investigated for this quasi-two-dimensional system. Interface states in the Bi/$Bi_{1-X}Sb_X$ heterojunction were considered in [4]. The aim of the present paper is to study the energy spectrum of the Bi–$Bi_{1-X}Sb_X$ compositional superlattices.

The paper is organized as follows. In section 2, information about the energy band structure of Bi and the $Bi_{1-X}Sb_X$ alloys is given.

In section 3 a dispersion equation for the energy spectrum of the Bi–$Bi_{1-X}Sb_X$ superlattices is derived. At the L point of the Brillouin zone the dispersion equation is obtained in the envelope function approximation within the McClure [5] model. The miniband spectrum of heavy holes at T and Σ is described by the standard dispersion equation obtained in the effective-mass approximation [6].

In section 4, calculations for superlattices with $X = 0.1$ and $X = 0.12$ are made. The effective mass of minibands, the Fermi energy and the concentration of free carriers in the superlattice with $X = 0.1$ and the period $d = 10$ nm are computed. The dependence of the miniband energy upon the ratio $r = d^{I}/d^{II}$ is obtained (d^{I} is the thickness of the Bi layers and d^{II} is the thickness of the alloy layers). It is shown that there is a transition from the semiconducting state ($r < 0.31$) to the semimetallic state ($r > 0.31$) due to an overlap between the minibands at the L and T points of the Brillouin zone. For $d^{I} = 4$ nm and $d^{II} = 6$ nm the Fermi surface of electrons is closed whereas the Fermi surface of holes is

0953-8984/94/102039+08$19.50

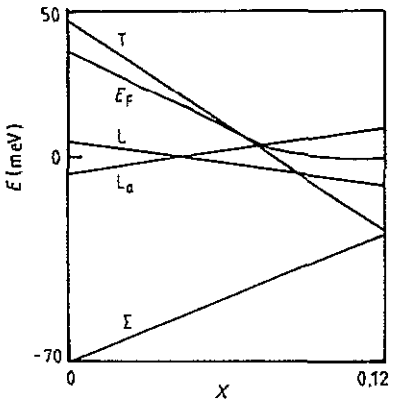

Figure 1. Transformation of the band structure of the $Bi_{1-X}Sb_X$ alloys with variation in the Sb content X (calculated according to [8–10]). The compositional dependence of the Fermi energy E_F obtained from a solution of the electroneutrality equation (3) is also shown.

open in the direction of the superlattice wavevector q. In the superlattice with $X = 0.12$ and $d^{I} = d^{II} = 60$ nm the transverse components of the effective-mass tensor change signs at a certain value of $q = q_0$. As a result, at $q > q_0$ the dependence of the miniband energy on the wavevector k in the plane of the layers has a shape like a 'camel's back'.

2. Energy band structure of Bi and $Bi_{1-X}Sb_X$

The semimetallic properties of Bi are due to the energy overlap between the conduction band L_s and the valence band T (L and T are the symmetry points in the Brillouin zone). An increase in the Sb content X of the $Bi_{1-X}Sb_X$ alloys is followed by inversion of the L_s and L_a bands (at $X = 0.04$) and a semimetal–semiconductor transition (at $X = 0.07$) due to the disappearance of the overlap between the L_a and T bands [7]. The valence band of the alloys ($X < 0.2$) contains light holes at L and heavy holes at T and Σ. The band edges at T and Σ vary linearly with X. According to [8,9],

$$E_T = 46.9 - 601.3X \qquad E_\Sigma = 359X - 70 \tag{1}$$

where the energy in units of millielectronvolts is counted from the middle of the energy gap at L. The gap value also depends on the Sb content linearly [10]:

$$E_{gL} = (10 - 242X)\ \text{meV}. \tag{2}$$

Transformation of the energy band structure with variation in the alloy composition in the range $0 \leqslant X \leqslant 0.12$ calculated on the basis of (1) and (2) is plotted in figure 1. In the figure the compositional dependence of the Fermi energy E_F obtained from solution of the electroneutrality equation

$$n_L = \rho_L + \rho_T + \rho_\Sigma \tag{3}$$

is also plotted.

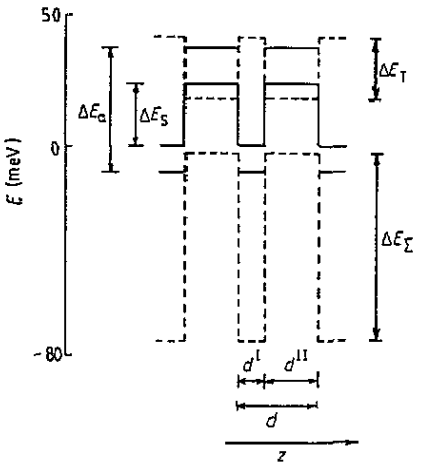

Figure 2. Diagram of the band-edge configuration for the Bi–$Bi_{1-X}Sb_X$ compositional superlattices. The energy is in units of millielectronvolts (the position of the bottom of the conduction band in Bi is taken as the energy zero). z is a direction perpendicular to the plane of layers. In the figure, ΔE_a and ΔE_s are the band-edge discontinuities at the L point of the Brillouin zone; ΔE_T and ΔE_Σ are the band-edge discontinuities at T and Σ, respectively, d^I is the thickness of the Bi layers and d^{II} is the thickness of the $Bi_{1-X}Sb_X$ layers.

The energy spectrum of heavy holes at Σ is described by the parabolic model with the density-of-states effective mass $m^\Sigma = 0.9m_0$ [9] (m_0 is the mass of a free electron). The spectrum of heavy holes at T is described by the same model with the effective-mass components [11] $m_x^T = m_y^T = 0.063m_0$ and $m_z^T = 0.667m_0$ (the z axis is directed along the trigonal C_3 axis). The energy spectrum at L is described by the McClure [5] model:

$$(E + 0.5E_{gL} + 0.5\alpha_{ay'y'}k_{y'}^2)(E - 0.5E_{gL} - 0.5\alpha_{sy'y'}k_{y'}^2) = Q_{xx}^2k_x^2 + Q_{y'y'}^2k_{y'}^2 + Q_{z'z'}^2k_{z'}^2. \tag{4}$$

Here the x axis is parallel to the binary C_2 axis, the y' axis is about $\phi_0 = 6°$ from the bisectrix axis and the z' axis makes an angle ϕ_0 with the trigonal C_3 axis; the Q_{jj} are defined by the velocity matrix elements, α_a and α_s are the free-electron and far-band contributions to the inverse band-edge effective mass of L_a and L_s, respectively, k is the wavevector and E is the energy taken from the middle of the gap E_{gL}. In the Sb content range $0 \leqslant X \leqslant 0.6$ [10], $Q_{xx} = 0.457 - 0.188X$, $Q_{y'y'} = 0.03 - 0.04X$, $Q_{z'z'} = 0.344$, $\alpha_{ay'y'} = 1.1 + 0.7X$, $\alpha_{sy'y'} = 0.615 + 0.4X$ (the values are given in atomic units). The tilt angle ϕ_0 decreases from 6° to zero with increasing Sb content ($0 \leqslant X \leqslant 0.7$) [8].

3. Band structure of the Bi–$Bi_{1-X}Sb_X$ superlattices

On the basis of results mentioned above in section 2, a diagram of the band-edge configuration for the Bi–$Bi_{1-X}Sb_X$ superlattices may be plotted. Let the position of the bottom of the conduction band in Bi be taken as the energy zero. A starting point for the construction of the diagram is the condition $\partial E_F/\partial z = 0$ throughout the superlattice in thermal equilibrium (z is the direction perpendicular to the plane of the layers). Owing to this condition the band edges in the $Bi_{1-X}Sb_X$ layer shift upwards by ΔE_F relative to

the position given in figure 1 (ΔE_F is the difference between the Fermi energy in Bi and that in $Bi_{1-x}Sb_x$). The energy band diagram for the Bi–$Bi_{0.9}Sb_{0.1}$ superlattices is plotted in figure 2.

At the L point the dispersion relation for the energy spectrum of the Bi–$Bi_{1-x}Sb_x$ superlattice is derived from solution of the Schrödinger equation using an effective Hamiltonian of the McClure [5] model and the approach developed in [12].

At low Sb concentrations, the changes in Q_{jj}, α_a and α_s are negligible compared with the discontinuity of the band edges in vicinity of the boundary between the layers. If the superlattice axis z is directed along the trigonal C_3 axis, the x axis is parallel to the binary C_2 axis and the y axis is parallel to the bisectrix axis (the tilt angle ϕ_0 may be neglected), the equation has the following form:

$$\begin{bmatrix} H_{11}-E & 0 & H_{13} & H_{14} \\ 0 & H_{11}-E & -H_{41} & H_{31} \\ H_{31} & -H_{14} & H_{33}-E & 0 \\ H_{41} & H_{13} & 0 & H_{33}-E \end{bmatrix} \begin{bmatrix} \chi_1(r) \\ \chi_2(r) \\ \chi_3(r) \\ \chi_4(r) \end{bmatrix} = 0. \tag{5}$$

Here the $\chi_j(r)$ are the envelopes of the wavefunction,

$$\begin{aligned} H_{11} &= E_a(z) - \alpha_{ayy}\hat{p}_y^2/2\hbar^2 \\ H_{33} &= E_s(z) + \alpha_{syy}\hat{p}_y^2/2\hbar^2 \\ H_{13} &= t\cdot\hat{p} \\ H_{31} &= t^*\cdot\hat{p} \\ H_{14} &= u\cdot\hat{p} \\ H_{41} &= u\cdot\hat{p} \end{aligned} \tag{6}$$

where $\hat{p} = -i\hbar\nabla$, t and u are the velocity matrix elements, and $E_a(z)$ and $E_s(z)$ are the band edges of L_a and L_s, respectively.

Equation (5) is equivalent to a set of four homogeneous differential equations. The substitution of these differential equations into each other leads to the effective equation

$$\{[(0.5\alpha_{ayy}\nabla_y^2 + E_a - E)(-0.5\alpha_{syy}\nabla_y^2 + E_s - E) + Q_{xx}^2\nabla_x^2 + Q_{yy}^2\nabla_y^2 + Q_{zz}^2\nabla_z^2]^2 + Q_{zz}^2(\partial E_a/\partial z)(\partial E_s/\partial z)\}\chi(r) = 0 \tag{7}$$

where $Q_{jj}^2 = \hbar^2(u_j^*u_j + t_j^*t_j)$.

Let the envelope function be chosen in the form

$$\chi(r) = \exp(ik_x x + ik_y y)\psi(z) \tag{8}$$

where

$$\psi^\mu(z) = A^\mu \exp(\kappa^\mu z) + B^\mu \exp(-\kappa^\mu z). \tag{9}$$

The superscript $\mu \equiv$ I, II marks the Bi layers ($\mu \equiv$ I) and the $Bi_{1-x}Sb_x$ layers ($\mu \equiv$ II). Let one of the boundaries be localized at the point $z = z_0$: the range $z_0 - d^I < z < z_0$

corresponds to the Bi layer with thickness d^{I} whereas the range $z_0 < z < z_0 + d^{\mathrm{II}}$ corresponds to the $Bi_{1-x}Sb_x$ layer with thickness d^{II}. In the range $z_0 - d^{\mathrm{I}} < z < z_0 + d^{\mathrm{II}}$ we may write

$$E_{\mathrm{a,s}}(z) = E^{\mathrm{I}}_{\mathrm{a,s}} + (E^{\mathrm{II}}_{\mathrm{a,s}} - E^{\mathrm{I}}_{\mathrm{a,s}})\theta(z - z_0). \tag{10}$$

In the vicinity of z_0, equation (7) has the form

$$\partial^2\psi/\partial z^2 = K\psi(z)\delta(z - z_0) \tag{11}$$

where

$$K^2 = (E^{\mathrm{II}}_{\mathrm{a}} - E^{\mathrm{I}}_{\mathrm{a}})(E^{\mathrm{I}}_{\mathrm{s}} - E^{\mathrm{II}}_{\mathrm{s}})/Q^2_{zz}. \tag{12}$$

Within the layer the equation for the envelope function has the form

$$\nabla^2_z\psi^\mu(z) = (\kappa^\mu)^2\psi^\mu(z) \tag{13}$$

where

$$(\kappa^\mu)^2 = [(0.5\alpha^\mu_{syy}k_y^2 + E^\mu_{\mathrm{s}} - E)(0.5\alpha^\mu_{ayy}k_y^2 - E^\mu_{\mathrm{a}} + E) + (Q^\mu_{xx}k_x)^2 + (Q^\mu_{yy}k_y)^2]/Q^2_{zz}. \tag{14}$$

The boundary condition for the envelope is

$$\psi^{\mathrm{I}}(z_0) = \psi^{\mathrm{II}}(z_0). \tag{15}$$

The boundary condition for the derivative of the envelope function can be obtained by integrating (11) with respect to z. The boundary condition for the derivative has the form

$$(\partial\psi/\partial z)_{z>z_0} - (\partial\psi/\partial z)_{z<z_0} = K\psi(z_0). \tag{16}$$

Let us write the boundary conditions (15) and (16) for the points $z = d^{\mathrm{II}}$ and $z = d$, where $d = d^{\mathrm{I}} + d^{\mathrm{II}}$ is the period of the superlattice. Then a set of homogeneous equations for the coefficients A^μ and B^μ may be derived if the Bloch condition

$$\psi^\mu(z + d) = \exp(\mathrm{i}qd)\psi^\mu(z) \tag{17}$$

is taken into account (q is the superlattice wavevector). The dispersion equation for the L-point energy spectrum of the superlattice is governed by the set determinant and has the form

$$\cos(qd) = \cosh(\kappa^{\mathrm{I}}d^{\mathrm{I}})\cosh(\kappa^{\mathrm{II}}d^{\mathrm{II}}) + 0.5[\kappa^{\mathrm{I}}/\kappa^{\mathrm{II}} + \kappa^{\mathrm{II}}/\kappa^{\mathrm{I}} - K^2/\kappa^{\mathrm{I}}\kappa^{\mathrm{II}}]\sinh(\kappa^{\mathrm{I}}d^{\mathrm{I}})\sinh(\kappa^{\mathrm{II}}d^{\mathrm{II}}). \tag{18}$$

The energy spectrum of heavy holes at T and Σ is described by the standard dispersion equation obtained in the effective-mass approximation [6]. For example, the dispersion equation for holes at T has the form

$$\cos(qd) = 0.5(\kappa^{\mathrm{II}}_{\mathrm{T}}/\kappa^{\mathrm{I}}_{\mathrm{T}} - \kappa^{\mathrm{I}}_{\mathrm{T}}/\kappa^{\mathrm{II}}_{\mathrm{T}})\sin(\kappa^{\mathrm{I}}_{\mathrm{T}}d^{\mathrm{I}})\sinh(\kappa^{\mathrm{II}}_{\mathrm{T}}d^{\mathrm{II}}) + \cos(\kappa^{\mathrm{I}}_{\mathrm{T}}d^{\mathrm{I}})\cosh(\kappa^{\mathrm{II}}_{\mathrm{T}}d^{\mathrm{II}}) \tag{19}$$

where

$$\begin{aligned}(\kappa^{\mathrm{I}}_{\mathrm{T}})^2 &= (m^{\mathrm{T}}_z/m^{\mathrm{T}}_x)k_x^2 + (m^{\mathrm{T}}_z/m^{\mathrm{T}}_y)k_y^2 - 2m^{\mathrm{T}}_z E/\hbar^2 \\ (\kappa^{\mathrm{II}}_{\mathrm{T}})^2 &= (m^{\mathrm{T}}_z/m^{\mathrm{T}}_x)k_x^2 + (m^{\mathrm{T}}_z/m^{\mathrm{T}}_y)k_y^2 + (2m^{\mathrm{T}}_z/\hbar^2)(\Delta E_{\mathrm{T}} - E).\end{aligned} \tag{20}$$

Here ΔE_{T} is the band-edge discontinuity at the T point (the energy is counted from the band edge in Bi).

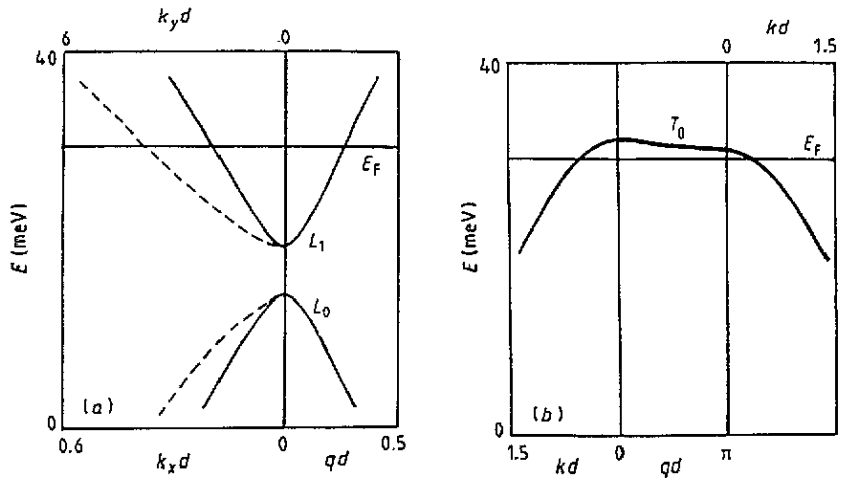

Figure 3. Energy spectrum of the Bi–$Bi_{0.9}Sb_{0.1}$ superlattice with the period $d = 10$ nm ($d^{I} = 4$ nm and $d^{II} = 6$ nm) (*a*) at the L point and (*b*) at the T point. The energy is counted from the bottom of the conduction band in Bi. The broken curves show the dependence of energy on the wavevector component k_y.

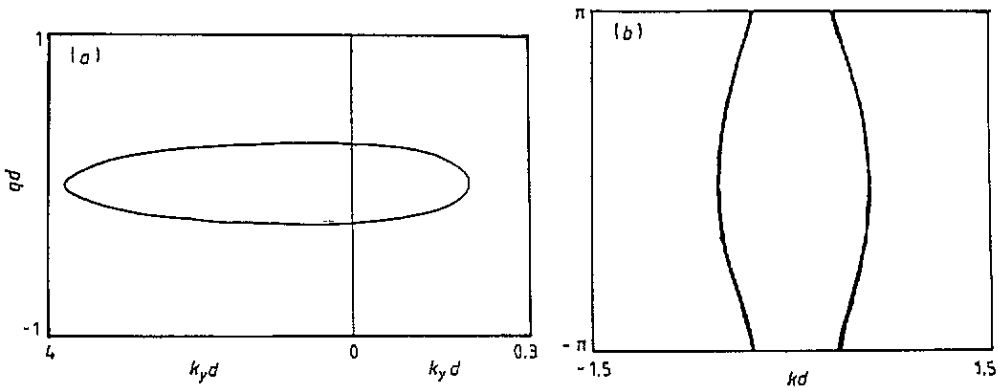

Figure 4. The Fermi surfaces of (*a*) electrons and (*b*) holes in the Bi–$Bi_{0.9}Sb_{0.1}$ superlattice with the period $d = 10$ nm ($d^{I} = 4$ nm and $d^{II} = 6$ nm).

4. Results of calculations for superlattices with $X = 0.1$ and $X = 0.12$

Figure 3 shows the energy spectrum of the Bi–$Bi_{0.9}Sb_{0.1}$ superlattice with $d = 10$ nm ($d^{I} = 4$ nm and $d^{II} = 6$ nm) calculated on the basis of (18) and (19). Calculations are made within the limits $E_s^{I} < E < E_a^{II}$. The energy distance between the minibands L_0 and L_1 is 4.5 meV. At the point L the density-of-states effective mass calculated by differentiating equation (18) has a value of $0.007m_0$. Overlap between the minibands L_1 and T_0 is 13.4 meV. The Fermi energy of electrons obtained from a solution of the electroneutrality equation at a temperature of 10 K is equal to 12 meV (the Fermi energy is taken from the bottom of miniband L_1). The concentration of free carriers is about 2×10^{16} cm^{-3}. The Fermi surfaces of electrons and holes are shown in figure 4. As one can see from the figure, the Fermi surface of electrons is closed whereas the Fermi surface

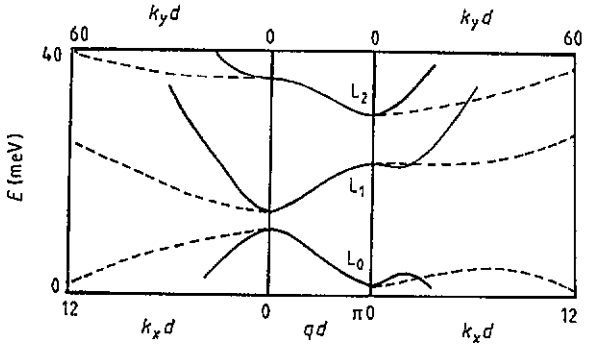

Figure 5. Energy spectrum of the Bi–$Bi_{0.88}Sb_{0.12}$ superlattice with the period $d = 120$ nm ($d^{I} = d^{II} = 60$ nm) at the L point. The energy is counted from the bottom of the conduction band in Bi. The broken curves show the dependence of energy on the wavevector component k_y.

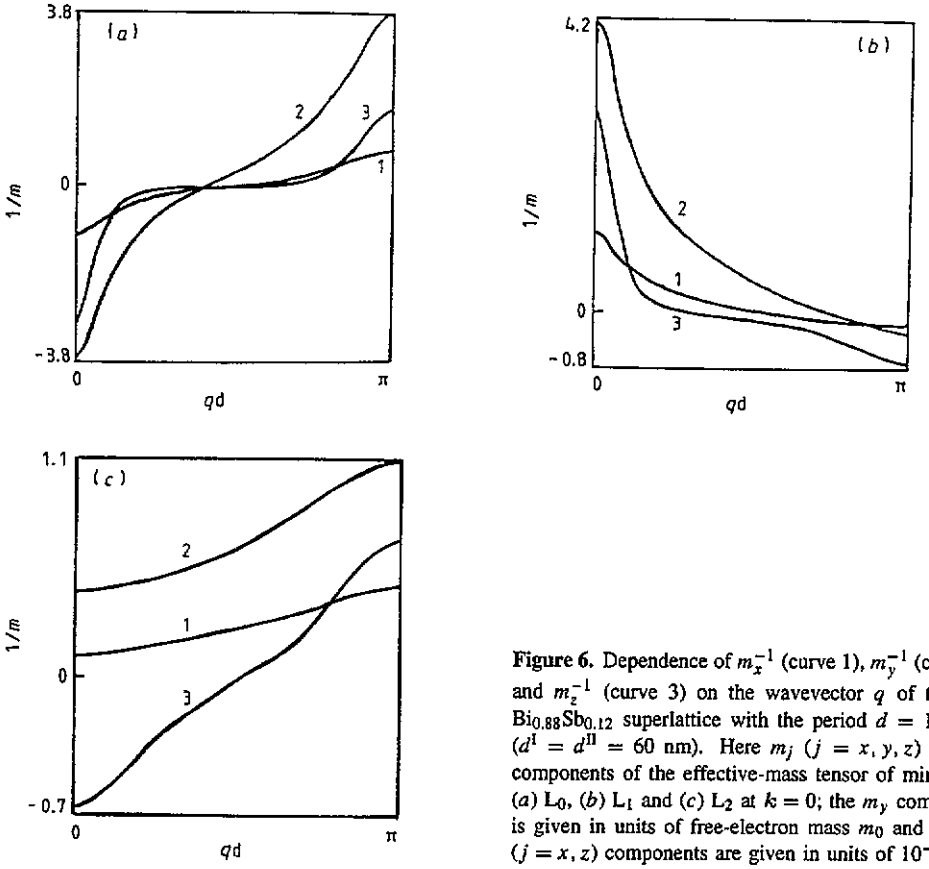

Figure 6. Dependence of m_x^{-1} (curve 1), m_y^{-1} (curve 2) and m_z^{-1} (curve 3) on the wavevector q of the Bi–$Bi_{0.88}Sb_{0.12}$ superlattice with the period $d = 120$ nm ($d^{I} = d^{II} = 60$ nm). Here m_j ($j = x, y, z$) are the components of the effective-mass tensor of minibands (*a*) L_0, (*b*) L_1 and (*c*) L_2 at $k = 0$; the m_y component is given in units of free-electron mass m_0 and the m_j ($j = x, z$) components are given in units of $10^{-3}m_0$.

of holes is open in the direction of the superlattice wavevector q and has the shape of a goffered cylinder.

The distance between the minibands L_0 and L_1 increases and reaches the value E_{gL}^{II};

the density-of-states effective mass at point L increases also but the overlap between the minibands L_1 and T_0 decreases with decreasing ratio $r = d^{I}/d^{II}$. Because of the disappearance of overlap at $r = 0.31$ there is a semimetal–semiconductor transition in the superlattice with $X = 0.1$ and $d = 10$ nm.

Calculations for superlattices with a period of about 100 nm show that the effective-mass components m_x and m_y of the minibands depend markedly on q. The energy spectrum of the $Bi–Bi_{0.88}Sb_{0.12}$ superlattice with $d^{I} = d^{II} = 60$ nm is shown in figure 5. In figure 6, the effective-mass components at $k = 0$ are plotted as a function of the wavevector q of this superlattice. As one can see from figure 6, the transverse components of the effective-mass tensor of the minibands L_0 and L_1 change signs at certain value of $q = q_0$. As a result, at $q > q_0$ the dependence of the miniband energy upon the wavevector k in the plane of the layers has a shape like a 'camel's back'.

5. Conclusions

Within the McClure model the energy spectrum of carriers in the $Bi–Bi_{1-X}Sb_X$ compositional superlattices in the envelope function approximation has been obtained. The Fermi surfaces of electrons and holes have been determined. Components of the effective-mass tensor have been calculated.

References

[1] Jalochowski M 1986 *Phys. Status Solidi* a **95** K5

[2] Borisova S S, Kondratenko V V, Ponomarev Ya G and Sudakova M V 1986 *Tez. Dokl. VI Vsesoyuzn. Simp. Plazma i neustoich. v Poluprov (Vilnius, 1986)* p 270 (in Russian)
Maliborskii P N and Ponomarev Ya G 1986 *Mater. VII Vsesoyuzn. Simp. Poluprov. s Uzkoi Zapr. Zonoi i Polumet. (Lvov, 1986)* vol 2, p 189 (in Russian)

[3] Aminov B A, Kondratenko V V, Ponomarev Ya G and Fedorenko A I 1988 *Tez. Dokl. XI Vsesoyuzn. Konf. po Fiz. Poluprov. (Kishinev, 1988)* vol 3, p 155 (in Russian)

[4] Agassi D and Chu T K 1987 *Appl. Phys. Lett.* **51** 2227

[5] McClure J W 1976 *J. Low Temp. Phys.* **25** 527
McClure J W and Choi K H 1977 *Solid State Commun.* **21** 1015
Dorofeev E A and Falkovsky L A 1984 *Zh. Eksp. Teor. Fiz.* **87** 2202

[6] Herman M A 1986 *Semiconductor Superlattices* (Berlin: Akademie)

[7] Mironova G A, Sudakova M V and Ponomarev Ya G 1980 *Fiz. Tverd. Tela* **22** 3628; *Zh. Eksp. Teor. Fiz.* **78** 1830

[8] Brandt N B, Herrmann R, Golysheva G I, Devyatkova L I, Kusnik D, Kraak V and Ponomarev Ya G 1982 *Zh. Eksp. Teor. Fiz.* **83** 2152

[9] Redko N A and Rodionov N A 1985 *Zh. Eksp. Teor. Fiz. Pis. Red.* **42** 246

[10] Brandt N B, Golysheva G I, Nguen Min Thu, Sudakova M V, Kashirin K N and Ponomarev Ya G 1987 *Fiz. Nizk. Temp.* **13** 1209
Brandt N B, Lavrenyuk M Yu, Minina N Ya and Savin A M 1988 *Zh. Eksp. Teor. Fiz.* **94** 235
Akhmedov S Sh, Herrmann R, Kashirin K N, Krapf A, Kraak V, Ponomarev Ya G and Sudakova M V 1990 *Zh. Eksp. Teor. Fiz.* **97** 663

[11] Dinger R J and Lawson A W 1973 *Phys. Rev.* B **7** 5215

[12] Volkov B A and Pankratov O A 1985 *Zh. Eksp. Teor. Fiz. Pis. Red.* **42** 145
Suris R A 1986 *Fiz. Tekh. Poluprov.* **20** 2008
Kantser V G and Lelyakov I A 1989 *Fiz. Tverd. Tela* **31** 235
Volkov B A and Karaganchu Yu V 1990 *Fiz. Tverd. Tela* **32** 2746
Kantser V G, Lelyakov I A and Malkova N M 1992 *Fiz. Tekh. Poluprov.* **26** 1596